



The absorption kinetics of NO in NaClO₂/NaOH solutions

Hsin Chu*, Tsung-Wen Chien, Bour-Wei Twu

Department of Environmental Engineering, National Cheng Kung University, Tainan, Taiwan, ROC

Received 31 October 2000; received in revised form 28 March 2001; accepted 30 March 2001

Abstract

A combined wet scrubbing SO_x/NO_x removal system is an advanced air pollution control process. In this process, the mechanism of NO removal is relatively unknown. Consequently, absorption of NO by alkaline solutions of NaClO₂ was studied to clarify the reaction kinetics. The experiments were carried out mainly at temperature 50°C which is the common operating temperature for wet scrubbers.

The assumption that the absorption occurred under the fast pseudo-*m*th reaction regime was verified in the experiments. The absorption rate of NO into NaClO₂ solutions was found to be proportional to $P_{\text{NO},0}^2$ and $[\text{NaClO}_2]_0^2$. The addition of NaOH to solutions of NaClO₂ decreased the absorption rate of NO. The absorption rate of NO at 25°C is lower than at 50°C. In the study, the absorption rate of NO did not change with changing gas flow rates. © 2001 Elsevier Science B.V. All rights reserved.

Keywords: Absorption; Reaction kinetics; Nitric oxide; Sodium chlorite; Stirred tank

1. Introduction

Acid rain is a major air pollutant caused by SO₂ and NO. Conventionally, engineers design separate air pollution control devices for each pollutant at high cost and space requirements. Combined SO₂/NO removal systems are, therefore, finding their niches. Among them, Makansi [1] indicated that a wet scrubbing combined SO₂/NO removal system was one of the best technologies for the job. The mechanism of SO₂ removal in the wet scrubbing is not new to us. However, the mechanism of NO removal in wet scrubbing has numerous unknown areas. In general, additives have to be added to the scrubbing system to convert insoluble NO to soluble NO_x or to form a complex, which can be removed.

* Corresponding author. Tel.: +886-6-2080108; fax: +886-6-2752790.
E-mail address: chuhsin@mail.ncku.edu.tw (H. Chu).

Nomenclature

[]	concentration in liquid phase (mol l^{-1})
D	diffusivity in liquid phase ($\text{cm}^2 \text{s}^{-1}$)
D	diffusivity in gas phase ($\text{cm}^2 \text{s}^{-1}$)
E	enhancement factor
I	ionic strength (g-ion l^{-1})
k	rate constant of (m, n)-order reaction ($(\text{l/mol})^{m+n-1} \text{s}^{-1}$)
k_G	gas-side mass transfer coefficient ($\text{mol s}^{-1} \text{cm}^{-2} \text{atm}^{-1}$)
k_L	liquid-side mass transfer coefficient (cm s^{-1})
N	absorption rate ($\text{mol s}^{-1} \text{cm}^{-2}$)
P	partial pressure (atm)
P_T	operating pressure of the system (atm)
P_W	saturated vapor pressure of water at operating temperature (atm)
X_a, X_c, X_g	contribution to K of anions, cations and the gas, respectively (l g-ion^{-1})

Subscripts

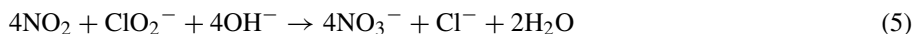
i	gas–liquid interface
w	water
0	initial value

Kobayashi et al. [2] investigated the removal of nitrogen oxides using a number of inorganic and organic reagents. Their results showed that the strong oxidizing reagents such as KMnO_4 and NaClO_2 removed NO efficiently. Chien and Chu [3] used $\text{NaClO}_2/\text{NaOH}$ to perform a preliminary test on a semi-continuous spraying sieve tray combined SO_2/NO removal system and a continuous spraying sieve tray column. The results showed that $\text{NaClO}_2/\text{NaOH}$ worked well for the combined SO_2/NO removal system. Chien et al. [4] also used a bench-scale spraying column to confirm the performance of NO_x removal with acidic NaClO_2 solutions. The NO conversion and NO_x removal efficiency increased with the increasing NO concentration, retention time, sodium chlorite concentration, operating temperature, and decreasing initial pH of the solution. As the sodium chlorite concentration exceeded than 0.4 M, the NO conversion and NO_x removal efficiency reached 100 and 80%, respectively. The NO conversion and NO_x removal efficiency at initial pH 4–7 were higher than that of initial pH > 7. Teramoto et al. [5] used a semi-batch stirred tank reactor to absorb NO in a $\text{NaClO}_2/\text{NaOH}$ solution to investigate the effect of various operating parameters on the absorption rate of NO. They found that the absorption rate of NO increased with the increasing NO concentration in the gas phase and the increasing NaClO_2 concentration in the liquid phase. However, their experiments were performed at 25°C , which is not the common operating temperature -50°C for wet scrubbers. Sada et al. [6–8] also carried out a series of NO, SO_2 , combined SO_2/NO absorption studies using NaClO_2 in a semi-batch stirred tank reactor. The concentrations of NO and SO_2 in the gas stream ranged from 0.15 to 15 vol.% and from 1.1 to 9.6 vol.%, respectively. Again, the experiments were performed at 25°C . They pointed out that NaClO_2 would be decomposed in an acid

solution as follows:



They also pointed out that the reaction of NO and NaClO₂ in an alkaline solution could be assumed as follows:



The rate of this reaction is regarded as the *m*th order relative to NO and the *n*th order relative to ClO₂⁻. Therefore, the absorption rate of NO can be expressed by Danckwerts [9]:

$$N_{\text{NO}} = \sqrt{\frac{2}{m+1}} k_{\text{DNO}} [\text{NO}]_i^{m+1} [\text{NaClO}_2]_0^n \quad (6)$$

Chan [10] investigated NO_x and SO₂ absorption. Experiments were conducted at room temperature and at near atmospheric pressure in 6 in. diameter column packed with 15.8 mm (5/8 in.) stainless steel Pall rings. Gas streams containing 150–1640 ppm NO_x or 500–3000 ppm SO₂ were scrubbed with water or sodium chlorite solutions. Up to 14% nitrogen oxide removal efficiency were obtained with water and 80% with sodium chlorite solutions with wide variation of chlorite concentration. A reaction mechanism had been proposed for the absorption of mixtures of NO and NO₂ found at typical flue gas levels. It is postulated that N₂O₃ is the major species involved when water scrubbing is employed. However, for absorption with NaClO₂ solution, NO is the major diffusing species.

Brogren et al. [11] investigated the absorption kinetics of NO into NaClO₂ solution using a packed column at 20°C. In the pH range 8–11, they found the reaction orders of NO and NaClO₂ were 1.3–1.8 and 0.6–0.9, respectively.

Hsu et al. [12] used a stirred tank with a plane gas–liquid interface at 30°C to investigate the absorption kinetics of lean NO with NaClO₂ solution. They found the reaction orders of NO and NaClO₂ were 2 and 1, respectively. The reaction rate constant in their result was $6.55 \times 10^8 \text{ (l/mol)}^2 \text{ s}^{-1}$.

Yang and coworkers [13–15] also conducted some experiments by bubbling or scrubbing various mixtures of NO, NO₂, O₂, and SO₂ with the balance N₂ into varying volumes of scrubbing solutions in bubbling column, spraying tower or packed chamber. Quantitative absorption of NO was achieved in nitric acid solutions containing chlorine gas, sodium hypochlorite, or sodium chlorite at atmospheric pressure and temperatures up to 80°C. They observed a greenish yellow color in the solution when scrubbing with acidic NaClO₂. The color was due to the presence of ClO₂ gas.

Absorptions of NO by alkaline solutions of NaClO₂ were performed in this study to clarify the reaction kinetics. The absorptions of diluted NO as encountered in flue gases into aqueous solutions of NaClO₂ and NaOH were carried out using a stirred vessel with a plane

gas–liquid interface at 50°C. Various operating parameters including NaClO₂ concentration, NaOH concentration, temperature, and gas flow rate were tested to determine the effect of these variables on the absorption kinetics of the reactants in both gas and liquid phases.

2. Experimental

The experimental setup and procedure were basically the same as in our previous investigation on the absorption kinetics of NO in the KMnO₄/NaOH solutions [16,17]; therefore, only a few essential features are repeated here.

2.1. Experimental setup

The system can be divided into three parts: a flue gas simulation system, an absorption reactor, and a gas sampling and analyzing system. Flow rates of N₂ and 2075 ppm NO were controlled by two mass flow meters. NO was diluted by N₂ in a plug flow mixer and further diluted, by the mass flow controlled compressed air in another plug flow mixer, to the desired concentrations and O₂ contents. The simulated flue gas was then heated to 50°C by a electrical heating tape before entering into the absorption reactor. The inner diameter and gas–liquid interfacial area of the stirred tank were 10 cm and 78.54 cm², respectively. The liquid volume and the gas volume in the tank were 770 and 580 cm³, respectively. The gas and liquid impellers were driven by two countercurrent variable speed DC motors, respectively. The heated simulation gas entered a saturator first to make sure it be saturated with water vapor. The tank was immersed in a water bath to keep the gas phase and liquid phase all at 50°C. The gas phase concentration of simulated flue gas in the inlet and outlet of absorber were measured by NO_x analyzer (Analysis Automation Limited model 441 chemiluminescent type), SO₂ analyzer (Signal series 1000 UV type), and O₂ analyzer (Signal Model 800 magneto dynamic type).

2.2. Materials

Standard gases included zero gas (N₂ 99.995%, San Fu), O₂ span gas (19%, San Fu), SO₂ span gas (4510 ppm, San Fu), and NO span gas (1010 ppm, San Fu). NaOH used was a product of Merck Chemical Inc. (purity > 99%) and NaClO₂ was a product of Nihon Isitu Chemical Inc. (purity > 87%).

2.3. Operational conditions and procedures

The operational conditions of the three experiments are given in Table 1. The simulated gas continuously flowed through the system with a flow rate of 2 l min⁻¹ and the liquid was not changed from its initial charge. Prior to the chemical absorption experiments, the physical absorption of CO₂ (99.8%, San Fu) into water was performed in the first experiment to determine the liquid-side mass transfer coefficients of the system. The absorption of diluted SO₂ (1000–3000 ppm) into an aqueous solution of 1 M NaOH was carried out in

Table 1

The operating conditions for various experiments involving liquid phase mass transfer, gas phase mass transfer, and NO absorption

Experiment number	P_{SO_2} (ppm)	P_{NO} (ppm)	$[\text{NaClO}_2]_0$ (M)	$[\text{NaOH}]_0$ (M)	n_L^a (rpm)	n_G^a (rpm)
1	–	–	–	–	80–330	237
2	1000–3000	–	–	1	208	160–300
3	–	300–800	0–1.5	0–0.3	208	237

^a Here, n_L is the agitation speed in liquid phase and n_G the agitation speed in gas phase.

the second experiment to determine the gas-side mass transfer coefficients of the system. In addition to these two experiments, a series of experiments were performed to measure NO absorption into NaClO₂/NaOH solutions to test the effects of various operating parameters on the absorption kinetics. Approximately, 20 ml each of the liquid sample of the first experiment was removed at the 5th and 10th minutes, respectively, for analysis. The analysis of the CO₂ concentration in the aqueous solution followed the standard titrimetric method. After a preliminary test was performed, the inlet and outlet gas samples were analyzed for all other experiments at the 10th and 12th minutes because that the absorption rate of the system remained stable after 6–7 min.

3. Results and discussion

3.1. Data analysis

The absorption rate of NO in the system, N_{NO} , measured in the experiments can be represented by [9]:

$$N_{\text{NO}} = k_G(P_{\text{NO},0} - P_{\text{NO},i}) = Ek_L([\text{NO}]_i - [\text{NO}]_0) \quad (7)$$

where $P_{\text{NO},0}$ can be obtained by

$$P_{\text{NO},0} = P_{\text{NO}}(P_T - P_W) \quad (8)$$

For a completely gas phase controlled reaction, e.g. $P_{\text{SO}_2,i} = 0$, N_{SO_2} can be simplified to

$$N_{\text{SO}_2} = k_G P_{\text{SO}_2,0} \quad (9)$$

$[\text{NO}]_{i,w}$, the interfacial concentration of NO in pure water, can be estimated from the Henry's law. However, the interfacial concentration of NO in an electrolyte solution, $[\text{NO}]_i$, is related to the ionic strength of the solution. Onda et al. [18,19] indicated that this was observed by Van Krevelen and Hoftijzer. The relation of them can be represented by

$$\log \left(\frac{[\text{NO}]_i}{[\text{NO}]_{i,w}} \right) = -(K_{\text{NaClO}_2} I_{\text{NaClO}_2} + K_{\text{NaOH}} I_{\text{NaOH}}) \quad (10)$$

where K_{NaClO_2} and K_{NaOH} are the salting-out parameters for the electrolyte NaClO_2 and NaOH , respectively. The salting-out parameter depends on the anions, cations, and gas present and is expressed by

$$K = X_a + X_c + X_g \quad (11)$$

Assuming the value of X is independent of temperature, the values of X for various species are available in the literatures of Sada et al. [20] and Onda et al. [18,19]:

$$X_a(\text{ClO}_2^-) = 0.3497, \quad X_a(\text{OH}^-) = 0.3875, \quad X_c(\text{Na}^+) = -0.0183, \\ X_g(\text{SO}_2) = -0.3145, \text{ and } X_g(\text{NO}) = -0.1825$$

$k_{\text{L,CO}_2}$ can be obtained from Eq. (7) with the data of the first experiment. The factor $k_{\text{G,SO}_2}$ can be obtained from Eq. (9) with the data of the second experiment. Sada et al. [7] indicated that $k_{\text{L,NO}}$ and $k_{\text{G,NO}}$ can be estimated by

$$k_{\text{L,NO}} = k_{\text{L,CO}_2} \left(\frac{D_{\text{NO-H}_2\text{O}}}{D_{\text{CO}_2\text{-H}_2\text{O}}} \right)^{2/3} \quad (12)$$

$$k_{\text{G,NO}} = k_{\text{G,SO}_2} \left(\frac{D_{\text{NO-N}_2}}{D_{\text{SO}_2\text{-N}_2}} \right)^{2/3} \quad (13)$$

where $D_{\text{CO}_2\text{-H}_2\text{O}}$ and $D_{\text{NO-H}_2\text{O}}$ can be calculated from the Wilke–Chang equation as shown in Bird et al.'s book [21] and the values of them are 3.59×10^{-5} and $4.47 \times 10^{-5} \text{ cm}^2 \text{ s}^{-1}$, respectively, at 50°C . $D_{\text{NO-N}_2}$ and $D_{\text{SO}_2\text{-N}_2}$ can be calculated from the Chapman–Enskog equation as shown in Bird et al.'s book [21] and the values of them are 0.234 and $0.147 \text{ cm}^2 \text{ s}^{-1}$, respectively, at 50°C .

3.2. $k_{\text{L,CO}_2}$ and $k_{\text{G,SO}_2}$

The liquid-side mass transfer coefficient, $k_{\text{L,CO}_2}$, for absorption of CO_2 into water is correlated with n_{L} (rpm) in this study by

$$k_{\text{L,CO}_2} = 7.12 \times 10^{-5} n_{\text{L}}^{0.578} \quad (14)$$

The gas-side mass transfer coefficient, $k_{\text{G,SO}_2}$ for absorption of diluted SO_2 into a solution with 1 M NaOH is correlated with n_{G} (rpm) in this study by

$$k_{\text{G,SO}_2} = 3.94 \times 10^{-6} n_{\text{G}}^{0.186} \quad (15)$$

3.3. $\text{NO}-(\text{NaClO}_2 + \text{NaOH})$ experiment

Fig. 1 shows the measurements of NO absorption rate over a range of NaClO_2 concentrations with 0.1 M NaOH . The observed absorption rate increases with the increasing concentration of NaClO_2 . The article of Sada et al. [6] and Danckwert's book [9] indicate that the reaction falls into fast pseudo- m th reaction regime if $1 \ll \sqrt{M} \ll E_i$, where \sqrt{M} is close to the fast reaction enhancement factor and E_i is the instantaneous enhancement

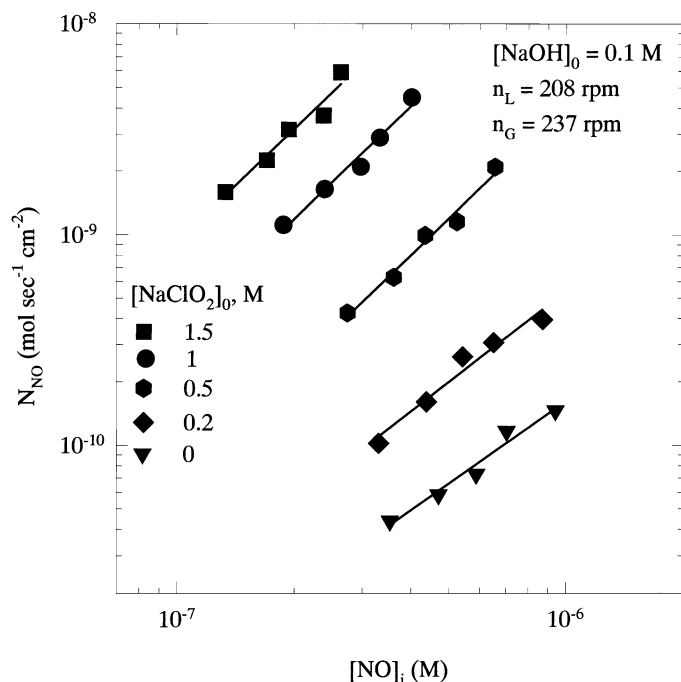


Fig. 1. Affect of gas–liquid interfacial NO concentration on the absorption rate of NO.

factor. The values of the enhancement factor and the instantaneous enhancement factor for this study are about several thousands and several millions, respectively. It meets the requirement of $1 \ll \sqrt{M} \ll E_i$. Therefore, the absorption rate of NO can be expressed by Eq. (6). From Fig. 1, there is a linear relationship between $\log N_{\text{NO}}$ and $\log [\text{NO}]_i$. Slopes of these lines are close to 1.5 while $[\text{NaClO}_2]_0 \geq 0.5 \text{ M}$, i.e. $(m + 1)/2 = 1.5$. This suggests that the reaction is second-order dependent on NO which is similar to Sada et al.'s results [6,7].

Fig. 2 shows the linear relationship of $\log N_{\text{NO}}$ and $\log [\text{NaClO}_2]_0$ for $[\text{NO}]_i = 2.5 \times 10^{-7} \text{ M}$, which is obtained by interpolating experimental data from Fig. 3. The slope of the straight line is close to 1.0, i.e. $n/2 = 1.0$. This suggests that the reaction is second-order dependent on NaClO_2 for this study. The average rate constant is $1.4 \times 10^6 (\text{l/mol})^3 \text{ s}^{-1}$ for cases of $[\text{NaClO}_2]_0 \geq 0.5 \text{ M}$. We could get the rate equation $N_{\text{NO}} = \sqrt{41.72[\text{NO}]_i^3 [\text{NaClO}_2]_0^2}$ by substituting the value of m , n , average rate constant and liquid phase diffusivity into Eq. (6). The liquid phase diffusivity of NO is $4.47 \times 10^{-5} \text{ cm}^2 \text{ s}^{-1}$.

Fig. 3 shows the measurements of NO absorption rate over a range of the NaOH concentrations with 0.5 M NaClO_2 . The observed absorption rate decreases with the increasing NaOH concentration. This result may be due to the presence of diluted NaOH inhibiting the production of ClO_2 which can help the oxidation of NO to more water soluble NO_2 [6,7].

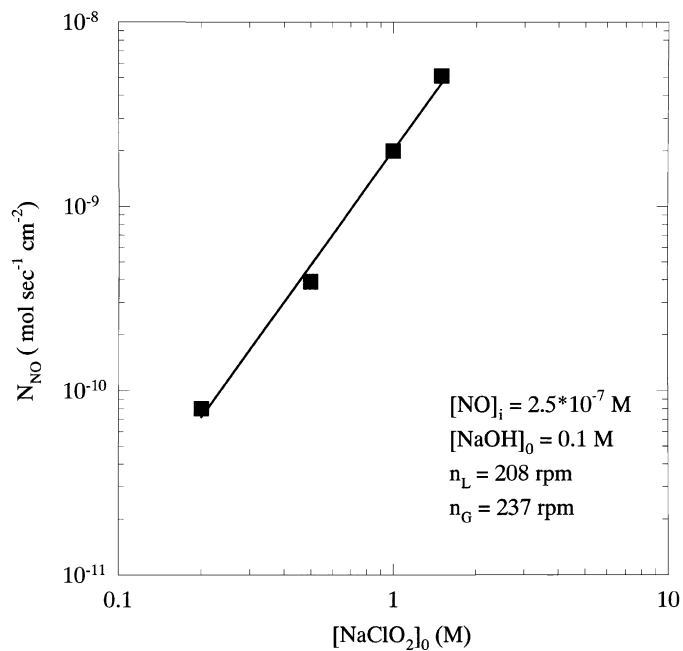


Fig. 2. Affect of $[\text{NaClO}_2]_0$ on the absorption rate of NO for a fixed value of $[\text{NO}]_i = 2.5 \times 10^{-7}$ M.

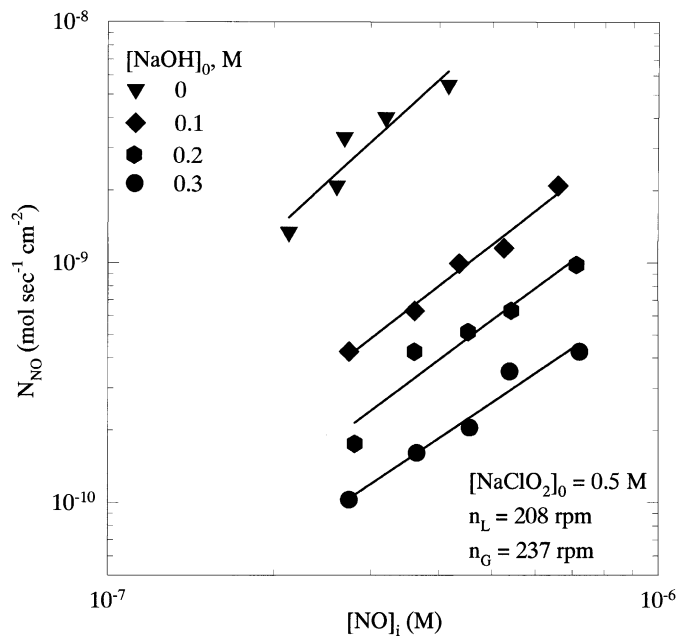


Fig. 3. Affect of $[\text{NaOH}]_0$ on the absorption rate of NO.

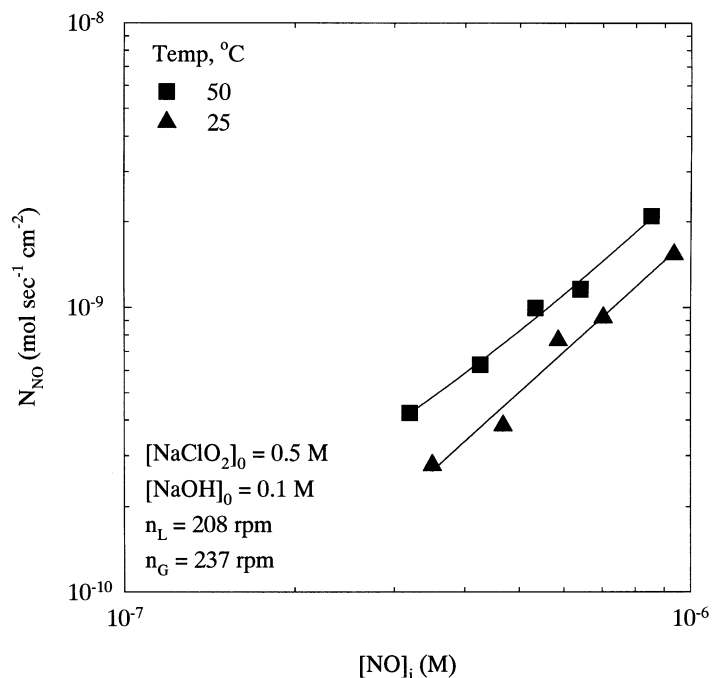


Fig. 4. Affect of operating temperature on the absorption rate of NO.

Fig. 4 shows the measurements of NO absorption rate over a range of the NO concentrations for various operating temperatures with 0.5 M NaClO₂ and 0.1 M NaOH. The observed absorption rate decreases with the decreasing temperature from 50 to 25°C. Although, the solubility of gases in liquid would increase as temperature decreases, however, the diffusivity of gases in liquid and reaction rate constants would decrease. Overall, this may cause the lower absorption rate of NO at 25°C.

Fig. 5 shows the measurements of NO absorption rate over a range of gas flow rates with 0.05 M NaClO₂ and 0.1 M NaOH. The observed absorption rate does not change much for various gas flow rates. This finding suggests that the absorption of NO in this study is not completely gas-film controlled.

Comparison of experimental results between this study and some previous studies are shown in Table 2. Under experimented conditions of 1000 ppm NO, 0.5 M NaClO₂, and 0.1 M NaOH, the absorption rates predicted from various researchers are also shown in Table 2. The absorption rate of this work is close to the results of Brogren et al. [10] and Hsu et al. [11], but markedly different from the results of Sada et al. [6,7]. The difference of the results between different researchers might be caused by the mass transfer limitations such as the different ranges of NO concentration in the simulated flue gas, NaClO₂ and NaOH concentration of the absorbing solutions, operating temperature, reactor geometry, etc.

Table 2
Comparison between the relevant studies of absorption kinetics of NO with NaClO₂ solutions

Reference	P_{NO} (ppm)	[NaClO ₂] ₀ (M)	[NaOH] ₀ (M)	pH	Temperature (°C)	Reaction order of NO (m)	Reaction order of NaClO ₂ (n)	Reaction rate constant k (l mol ⁻¹) $m+n-1$ s ⁻¹	Reaction rate ^a
6	0.8–15 vol.%	0.2–1.5	0.05–0.5	–	25	2	1	$3.8 \times 10^{12} \text{ exp}(-3.73[\text{NaOH}]_0)$	1.2×10^{-5}
7	0.5–7.5%	0.29–1.64	0.015	–	25	2	1	2.1×10^{12}	8.8×10^{-6}
11	200–1000	0.05–1.0	–	9.2–9.9	30	2	1	6.55×10^8	1.6×10^{-7}
12	290	0.1–1.0	–	8	20	1.766	0.693	1.55×10^6	4.4×10^{-8}
			–	9	20	1.665	0.603	1.40×10^6	8.8×10^{-8}
			–	10	20	1.553	0.668	3.80×10^5	9.9×10^{-8}
			–	11	20	1.346	0.908	1.22×10^4	7.2×10^{-8}
This work	300–800	0.0–1.5	0.0–0.3	–	50	2	2	1.39×10^6	5.1×10^{-9}

^a $P_{\text{NO}} = 1000$ ppm, [NaClO₂]₀ = 0.5 M, [NaOH]₀ = 0.1 M.

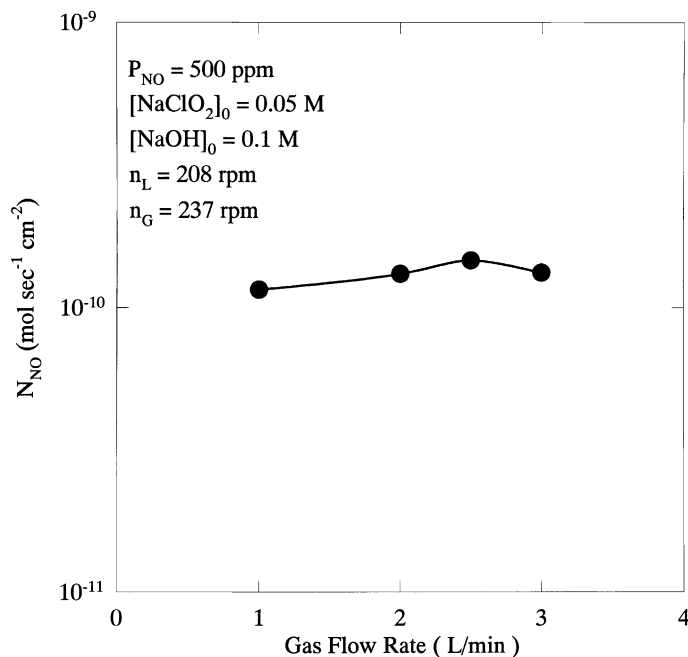


Fig. 5. Affect of gas flow rate on the absorption rate of NO.

4. Conclusions

According to the assumption that the absorption was developed under the fast-reaction regime, the absorption rate of NO into NaClO₂ solutions was found to be proportional to $P_{\text{NO},0}^2$ and $[\text{NaClO}_2]_0^2$. The addition of NaOH into the solution of NaClO₂ would decrease the absorption rate of NO. The absorption rate of NO at 25°C is lower than that of 50°C. In the range of this study, the absorption rate of NO would not change by changing the gas flow rate.

Acknowledgements

This study was funded in part by National Science Council, Republic of China (NSC 84-2211-E-006-001).

References

- [1] T. Makansi, Power 9 (1990) 26.
- [2] H. Kobayashi, N. Takezawa, T. Niki, Environ. Sci. Technol. 11 (1977) 190.
- [3] T.W. Chien, H. Chu, J. Hazardous Mater. 80 (2000) 43.
- [4] T.W. Chien, H. Chu, H.T. Hsueh, J. Environ. Sci. Health A36 (2001), in press.

- [5] M. Teramoto, M. Ikeda, H. Teranishi, *Jpn. Chem. Eng.* 2 (1976) 637 (in Japanese).
- [6] E. Sada, H. Kumazawa, I. Kudo, T. Tondo, *Chem. Eng. Sci.* 33 (1978) 315.
- [7] E. Sada, H. Kumazawa, Y. Yamanaka, I. Kudo, T. Kondo, *J. Chem. Eng. Jpn.* 11 (1978) 276.
- [8] E. Sada, H. Kumazawa, I. Kudo, T. Kondo, *IEC Process Des. Dev.* 18 (1979) 275.
- [9] P.V. Danckwerts, *Gas-Liquid Reaction*, McGraw-Hill, New York, NY, 1970.
- [10] K.F. Chan, *Experimental Investigation and Computer Simulation of NO_x and SO_x Absorption in a Continuous-Flow Packed Column*, Ph.D. Dissertation, Department of Chemical Engineering, University of Windsor, Ont., Canada, 1991.
- [11] C. Brogren, H.T. Karlsson, I. Bjerle, *Chem. Eng. Technol.* 21 (1998) 61.
- [12] H.W. Hsu, C.J. Lee, K.S. Chou, *Chem. Eng. Comm.* 170 (1998) 67.
- [13] C.L. Yang, *Aqueous Absorption of Nitrogen Oxides Induced by Oxychlorine Compounds: A Process Development Study for Flue Gas Treatment*, PhD Thesis, Department of Chemical Engineering, Chemistry and Environmental Science, New Jersey Institute of Technology, 1994.
- [14] C.L. Yang, H. Shaw, H.D. Perlmutter, *Chem. Eng. Commun.* 143 (1996) 23.
- [15] C.L. Yang, H. Shaw, *Environ. Prog.* 17 (1998) 80.
- [16] H. Chu, S.Y. Li, T.W. Chien, *J. Environ. Sci. Health A33* (1998) 801.
- [17] H. Chu, T.W. Chien, S.Y. Li, *Sci. Total Environ.* 275 (2001) in press.
- [18] K. Onda, E. Sada, T. Kobayashi, S. Kito, K. Ito, *J. Chem. Eng. Jpn.* 3 (1970) 18.
- [19] K. Onda, E. Sada, T. Kobayashi, S. Kito, K. Ito, *J. Chem. Eng. Jpn.* 3 (1970) 137.
- [20] E. Sada, H. Kumazawa, H. Hikosaka, *IEC Fundamental* 25 (1986) 386.
- [21] R.B. Bird, W.E. Stewart, E.N. Lightfoot, *Transport Phenomena*, Wiley, New York, NY, 1960.